Applied Catalysis B: Environmental 156–157 (2014) 101–107

Contents lists available at ScienceDirect

Applied Catalysis B: Environmental

journal homepage: www.elsevier.com/locate/apcatb

Oxidative degradation of phenanthrene in the absence of light irradiatiion by hybrid ZrO_2-acetylacetonate gel-derived catalyst

Filomena Sannino[a], Domenico Pirozzi[b], Giuseppe Vitiello[c,d], Gerardino D'errico[c,d], Antonio Aronne[b], Esther Fanelli[b], Pasquale Pernice[b,*]

[a] Università di Napoli Federico II, Dipartimento di Agraria, Via Università 100, I-80055 Portici (Na), Italy
[b] Università di Napoli Federico II, Dipartimento di Ingegneria Chimica, dei Materiali e della Produzione Industriale, P.le Tecchio 80, I-80125 Napoli, Italy
[c] Università di Napoli Federico II, Dipartimento di Scienze Chimiche, Complesso Universitario Monte Sant'Angelo, Via Cinthia, I-80126 Napoli, Italy
[d] Consorzio Interuniversitario per lo Sviluppo dei Sistemi a Grande Interfase, Unità di Napoli, Complesso Universitario Monte Sant'Angelo, Via Cinthia, I-80126 Napoli, Italy

ARTICLE INFO

Article history:
Received 25 December 2013
Received in revised form 25 February 2014
Accepted 4 March 2014
Available online 13 March 2014

Keywords:
Acetylacetonate complex
Phenanthrene
ZrO_2 Xerogel
Hybrid material
EPR

ABSTRACT

The intrinsic catalytic activity of a hybrid gel-derived ZrO_2-acetylacetonate (HSGZ) material towards the oxidative degradation of phenanthrene (PHE), in aqueous solution and in the dark, was revealed for the first time.

The HSGZ catalyst is a polymeric network of zirconium oxo-clusters on the surface of which part of Zr^{4+} ions are involved in strong complexation with acetylacetonate (*acac*) ligands. The HSGZ gave significant PHE degradation rates acting as radicals initiator without any light irradiation at 30 °C.

Free radicals were formed on the solid surface by the coexistence of Zr(IV)-*acac* and Zr(III)-*acac*• complexes in equilibrium at a given temperature, from which reactive oxygen species were produced in the presence of molecular O_2. A direct evidence of radical's presence on HSGZ solid surface was obtained by EPR spectroscopy.

The analysis of the degradation products confirmed that the reaction goes on through the formation of intermediate free radicals, leading to the first ring-opening and to the formation of phthalates as main intermediates. Subsequently, low molecular weight alkanes are produced. Finally, a deep oxidation of the intermediates occurs completing the mineralization process. The HSGZ catalyst showed a good stability under the reaction conditions, retaining its catalytic activity after repeated tests.

1. Introduction

The increase of industrial development, population growth and urbanization has promoted the release of hazardous chemicals in the environment and a general global pollution. Polycyclic aromatic hydrocarbons (PAHs), ubiquitous environmental contaminants found in air, soil and waters, have toxic, genotoxic, carcinogenic and mutagenic effects [1,2]. PAHs exhibit high stability and low water solubility due to the delocalization of π-electrons, leading to their accumulation in food chains, so threatening human health and environment quality [3]. Therefore, the removal of PAHs and the development of effective strategies to remediate polluted sites is a current focus of research in the environmental science.

In the last decades many attempts have been made to remove PAHs from the environment. Traditional chemical or physical technologies, such as sorption [4] or treatment with oxidants [5], have inherent drawbacks due to operating costs, operational problems and production of secondary pollutants [6,7]. On the other hands, the low solubility of these organic compounds hampers the bioremediation techniques [8] such as phytoremediation [9] or biodegradation by fungi or bacteria [5]. To date, the development of an effective method for PAHs degradation still remains a challenge.

In the recent years, photocatalysis by either solar energy or artificial light has emerged as one of the most attractive strategies for PAHs degradation. Heterogeneous photocatalysis offers an oxidative process capable of pollutant removal under ambient conditions via irradiation of some semiconductor solids [10] which can be used as photocatalysts suspended in the water effluent, or immobilized on different types of supports [11]. To date, most of the studies concern TiO_2 [12] due to its stability and its relatively high

* Corresponding author. Tel.: +39 081 7682411; fax: +39 081 7682595.
E-mail address: pernice@unina.it (P. Pernice).

http://dx.doi.org/10.1016/j.apcatb.2014.03.006
0926-3373/

activity, though the band gap of TiO_2 is so large that it can only utilize less than 5% of solar energy. As a result, current interests are directed toward the application of photocatalysts that work under visible light irradiation to efficiently utilize sunlight. Kou et al. [13] showed that the oxidation reactions of five typical PAHs, carried out by using tantalum oxynitride and Pt-tantalum oxynitride, are driven only by the presence of visible radiation, so confirming the great importance of light in this process as reported in the literature [14–16].

In the present paper, we demonstrate for the first time the intrinsic catalytic activity of a gel-derived hybrid zirconia material (HSGZ) toward the phenanthrene (PHE) oxidative degradation in aqueous solution. This catalyst gives high PHE degradation rate acting as a radical initiator without any light irradiation. Phenanthrene is among the 16 PAHs listed as primary pollutants by US Environmental Protection Agency (EPA) [17] and it is known to be a human skin photosensitizer and mild allergen [18]. It is a typical three-ring PAH and has been used as a model compound to test the catalytic activity of HSGZ material in pollutants degradation.

The HSGZ material previously synthesized [19,20] is a class II hybrid ZrO_2-acetylacetone gel-derived material; after drying at low temperature HSGZ xerogel holds the acetylacetone used in the sol–gel synthesis and can be considered as an *acac* surface-modified porous zirconia. The catalyst ability to produce free radicals in absence of irradiation has been ascertained by EPR spectroscopy and related to the presence of the *acac* ligands on HSGZ surface. Kinetics of PHE removal was evaluated and a two-steps kinetic model has been proposed.

2. Experimental

Phenanthrene (99.0% purity) was purchased from Sigma–Aldrich (UK). All solvents were of HPLC grade (Carlo Erba, Italy) and were used without further purification.

The hybrid sol–gel zirconia (HSGZ) was prepared according to the procedure elsewhere reported [19]. A solution containing 10 mL of zirconium(IV) propoxide (70 wt.% in 1-propanol) (22.6 mmol), 1.5 mL of acetylacetone (99+%) (14.6 mmol) and 3.0 mL of 1-propanol (99.80+%) (39.9 mmol) was prepared and stirred at room temperature for a few minutes. A second solution containing 3.0 mL of distilled water (166 mmol) and 5.5 mL of 1-propanol (73.2 mmol) was added to the first one. The solution obtained was vigorously stirred for about 20 min at room temperature, until the gelation occurred. A homogeneous slightly yellow colored gel was obtained. The gel was left at room temperature for 24 h and then lyophilized at −50 °C for 20 h to obtain the porous amorphous material (about 300 m^2/g) [21]. A reference ZrO_2 matrix (SGZ) was also prepared in similar conditions except for the lack of acetylacetone in the solution of the Zr precursor. Consequently, when the hydro-alcoholic solution was added to the precursor solution, the instantaneous formation of a particulate gel took place.

Gel-derived zirconia material, HSGZ, has been characterized by Electron Paramagnetic Resonance (EPR). The powder sample was analyzed using an X-band (9 GHz) Bruker Elexys E-500 spectrometer (Bruker, Rheinstetten, Germany). The capillary containing the sample was placed in a standard 4 mm quartz sample tube. The temperature of the sample was regulated at 25 °C and maintained constant during the measurement by blowing thermostated nitrogen gas through a quartz Dewar. The instrumental settings were as follows: sweep width, 100 G; resolution, 1024 points; modulation frequency, 100 kHz; modulation amplitude, 1.0 G; time constant, 20.5 ms. EPR spectra were measured with attenuation of 10 dB to avoid microwave saturation of resonance absorption curve. Several scans, typically 64, were accumulated to improve the signal-to-noise ratio. The *g* values were evaluated by means of two internal standards (1,1-diphenyl-2-picrylhydrazyl (DPPH) and a 4-hydroxy-2,2,6,6-tetramethylpiperidin-1-oxyl (TEMPOL) ethanol solution) which were inserted in the quartz sample tube co-axially with the capillary containing the HSGZ sample [22].

A stock aqueous solution of PHE 0.8 mg L^{-1} was prepared and subsequently it was kept refrigerated in the dark to avoid photocatalytic degradation reactions. Blanks of PHE in aqueous solution were analyzed in order to check its stability and the possible sorption to vials. The PHE removal was studied as a function of the solid/liquid ratio R (R = mg of matrix/1 mL of PHE aqueous solution). The following ratios were used: R = 0.1, 0.4, 0.6, 0.8, 1.0, 2.0, 5.0 and incubation time of 60 min. All the tests were carried out in the dark to avoid any additional photocatalytic degradation. After incubation in a thermostatic rotary shaker at 30 °C, the samples were centrifuged at 10,000 rpm for 10 min and the supernatants were analyzed as described below. The percentage removal of PHE (X) was calculated by the following equation:

$$X = \frac{c_0 - c}{c_0} \times 100 \quad (1)$$

where c_0 and c are the concentrations of PHE (mg L^{-1}) at the start and at the end of the incubation, respectively.

Kinetic tests in the presence of HSGZ matrix at R = 0.4 were performed fixing incubation times of 5, 10, 15, 30, 60, 120, 360 and 1440 min at 30 °C.

The long-term applicability of the PHE-removal system was verified by carrying out repeated batch tests at R = 10 and after 1 h of incubation time. After each batch test, the liquid phase was removed and replaced by an equal volume of PHE solution at the initial concentration of 0.8 mg L^{-1}.

Analytical determination of PHE was performed by an Agilent 1200 HPLC apparatus (USA), equipped with a DAD and a ChemStation Agilent Software. A Macharey-Nagel Nucleosil 100-5 C18 column (stainless steel 250 mm × 4 mm) was utilized. The mobile phase, a binary system of 85:15 acetonitrile: water, was pumped at 1 mL min^{-1} flow in isocratic mode. The detector was set at 252 nm and the injection volume was 20 μL. The quantitative determination of PHE was performed using a calibration curve between 0.05 and 0.8 mg L^{-1}.

The PHE degradation products were extracted and identified by Gas Chromatography-Mass Spectrometry (GC-MS) analysis. In a typical experiment, 5 mL of PHE aqueous solution (0.8 mg L^{-1}) was incubated with 50 mg of HSGZ for 1 and 24 h, respectively. After reaction, the slurry of reaction mixture was taken out and centrifuged to remove the HSGZ solid. The collected supernatants were extracted in a separatory funnel with *n*-hexane in the ratio 1:6 (v:v). This procedure was repeated by three times to assure all of PHE degradation products were extracted. The *n*-hexane layer was dried by anhydrous sodium sulphate, evaporated under reduced pressure at 30 °C and dissolved in 1 mL of dichloromethane phase before GC-MS analysis.

The samples were analyzed using a Perkin-Elmer AutoSystem™ XL gas chromatograph, equipped with a Programmed-Temperature Split/Splitless injector with programmable pneumatic control kept at a constant temperature of 250 °C, a Restek Rtx-5MS capillary column (5% diphenyl-95% dimethylpolysiloxane, length 30 m, 0.25 mm ID, and 0.25 μm df), and a Perkin-Elmer TurboMass Gold mass-spectrometer. The oven temperature was programmed to run at 60 °C for 5 min and then to increase by 15 °C min^{-1} to a final temperature of 280 °C. Under these conditions the retention time for PHE was 12.75 min. A NIST mass spectral library version 1.7 was used for peak identification. All the experiments were performed in triplicate and the relative standard deviation was lower than 4%.

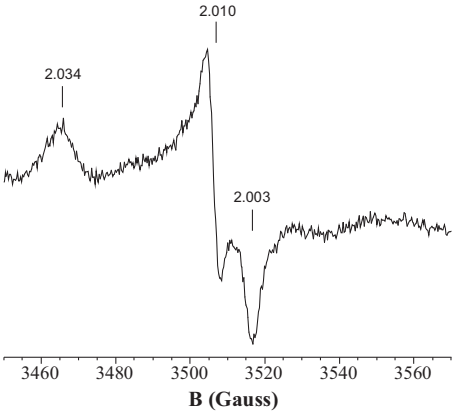

Fig. 1. EPR spectrum of HSGZ sample recorded at room temperature, *g* values are reported.

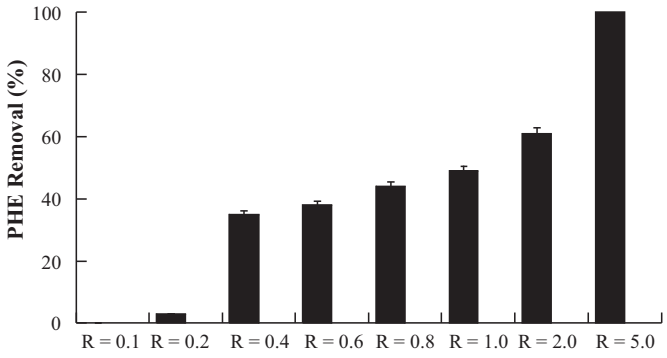

Fig. 2. PHE percentage removal after 1 h incubation time as function of solid/liquid ratio *R*.

3. Results

In order to reveal the presence of paramagnetic species, the gel-derived zirconia material (HSGZ), used as catalyst for the phenanthrene (PHE) oxidative degradation in aqueous solution, has been characterized by EPR spectroscopy. Each measurement was repeated after 12 h leaving the sample in the sample-holder of the spectrometer to avoid any light exposure. The spectrum of the HSGZ powder recorded at room temperature is reported in Fig. 1 and presents a complex anisotropic lineshape that is correlated to the presence of stable radicals adsorbed on the HSGZ surface.

EPR spectra were also recorded on HSGZ samples that have been used 1 and 24 h as catalyst in PHE degradation reaction. These spectra look not much different respect to that of Fig. 1 meaning that HSGZ material is stable in the reaction conditions.

The PHE removal tests were performed at 30 °C in a stirred batch system in dark condition. Each test was started introducing a fixed amount of HSGZ (from 0.1 to 5 mg) in 1 mL of PHE aqueous stock solution (0.8 mg L^{-1}). All the tests were carried out in a 10 mL capped test tube. The inside air volume assured an oxygen reservoir, largely exceeding the stoichiometric amount required for the full oxidation of PHE to CO_2 and H_2O. Therefore, the tests can be considered as made at constant O_2 concentration. The fractions of PHE removed after an incubation time of 60 min are reported in Fig. 2 as a function of the solid/liquid ratio R.

The experimental results show that a virtually complete removal of PHE was achieved adopting a solid/liquid ratio $R = 5.0$. A shorter incubation time (15 min) was required for the total removal of PHE at a higher solid/liquid ratio ($R = 10$).

The formation of PHE degradation products is demonstrated by the data in Fig. 3, that display the total ion chromatogram (a) and the mass spectrum of peak at retention time (RT) 19.65 min (b), obtained after incubation of a PHE solution over HSGZ for 1 h at $R = 10$. According to the standard spectra in NIST 1.7 library data, the peak at RT of 19.65 min could be assigned to bis(2-ethylhexyl)phthalate compound as confirmed by the standard spectra (c). Similarly, the peak at RT of 7.26 min could be identified as 1-dodecanol-2 methyl compound belonging to the class of alkanols, the ones at 12.09, 12.94, 13.74, and 14.51 min attributable

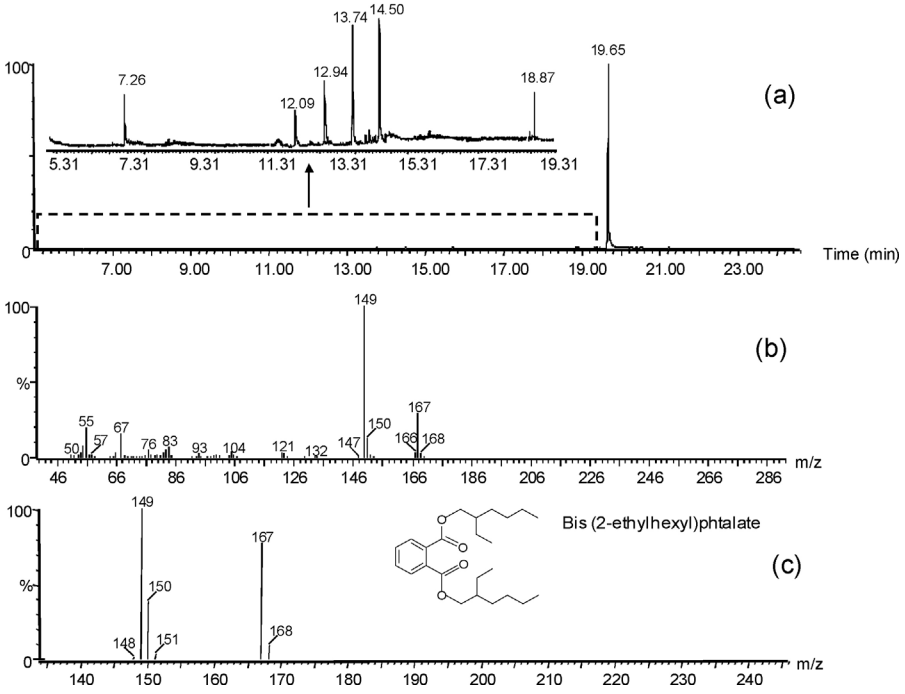

Fig. 3. PHE catalytic degradation after 1 h incubation time and $R = 10$: (a) total ion chromatogram; (b) mass spectrum of the peak at RT 19.65 min, (c) standard spectra of RT 19.65.

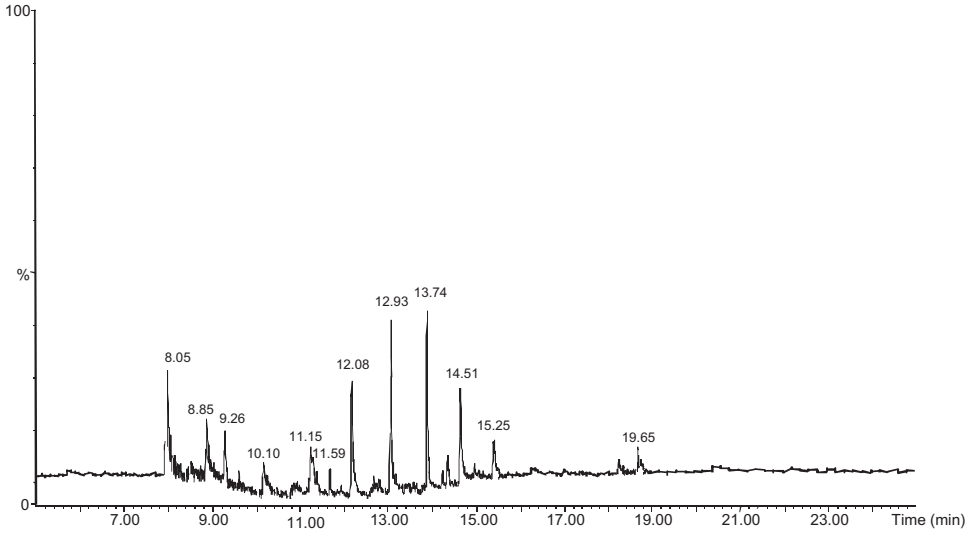

Fig. 4. Total ion chromatogram of PHE catalytic degradation products after 24 h incubation time and $R = 10$.

to different alkanes and finally the one at 18.87 min as hexanedioic acid, bis (2-ethylhexyl) ester compound.

Similar measurement were carried out after the incubation of a PHE solution over HSGZ for 24 h at $R = 10$ (Fig. 4). In this case, the degradation products were represented by bis(2-ethylhexyl)phthalate compound (RT 19.65) in undetectable concentration and by an amount of alkanes that was significantly increased in comparison to that observed after 1 h, becoming the major product.

To clarify the role of the organic components of the HSGZ matrix in the PHE removal, experiments were carried out incubating 10 mg of SGZ matrix (i.e., the matrix not containing *acac* ligand) with 1 mL of a 0.8 mg L^{-1} solution of PHE for 60 min. Although a considerable removal was observed (62%), no degradation products were detected, indicating that in this case the removal occurred only by a sorption mechanism. Anyway, it is worth to note that with the same $R = 10$ value HSGZ gave 100% in only 15 min.

The kinetics of PHE degradation in the presence of HSGZ catalyst was evaluated at 30 °C and $R = 0.4$. In Fig. 5 the residual concentration of PHE in the solution (C_{sol}) is reported as a function of the reaction time (t) showing a significant PHE removal. The experimental data indicate that, after a relatively fast initial decrease of the PHE concentration in the liquid solution, the removal of the remaining amount of dissolved PHE occurred at reduced rate, suggesting that PHE removal was triggered by two different mechanisms. The concentration–time profile in Fig. 5 could be interpolated using a double-exponential model:

$$C_{sol}(t) = Ae^{-\lambda_1 t} + Be^{-\lambda_2 t} \quad (2)$$

The estimates of the parameters of the mathematical model (2) are reported in Fig. 5.

In order to evaluate the operational stability of the HSGZ in the presence of PHE, repeated batch experiments were performed at $R = 10$ and after 1 h of incubation time. The liquid phase was removed after each batch and replaced by an equal volume of PHE solution at the initial concentration of 0.8 mg L^{-1}. The conditions chosen for this test allow working at high removal rate, as previously said with $R = 10$ complete PHE removal was achieved in 15 min.

The results shown in Fig. 6 demonstrate that, as subsequent batches were carried out, the removal efficiency of HSGZ decreased from 100% until a constant asymptotic level (about 80%) was reached after 6 repeated batches.

4. Discussion

The ZrO_2-acetylacetonate hybrid material (HSGZ) used as catalyst in this work was prepared by a sol–gel synthesis starting from zirconium(IV) propoxide and using acetylacetone (*Hacac*) to stabilize the sol, thus controlling the reactivity of the zirconium precursor. Depending on the *Hacac*/Zr ratio, different heteroleptic alkoxide-*acac* complexes were formed [23,24]. These complexes

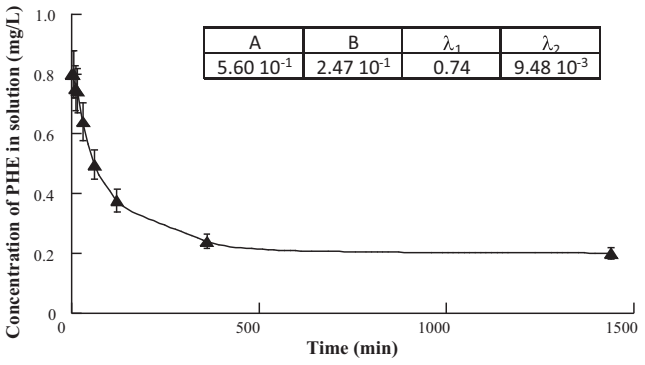

Fig. 5. Kinetics of PHE removal in the presence of HSGZ catalyst. $T = 30$ °C, $R = 0.4$. The model (2) was used to find the regression curve. The estimates of the parameters of model (2) are reported in the inset.

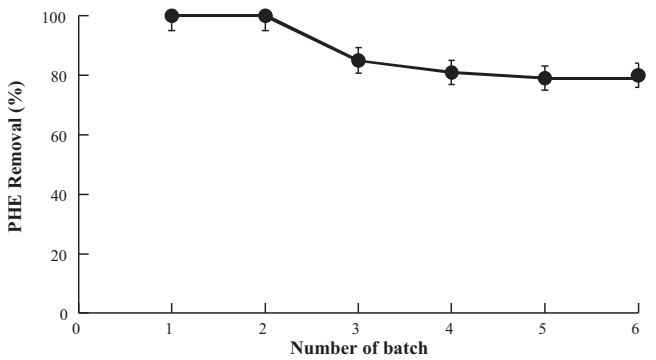

Fig. 6. PHE removal by repeated batch in the presence of HSGZ catalyst. $T = 30$ °C, $R = 10$.

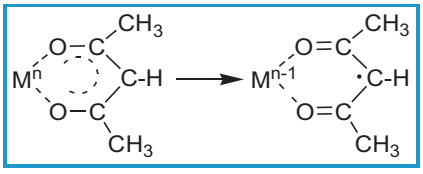

Scheme 1.

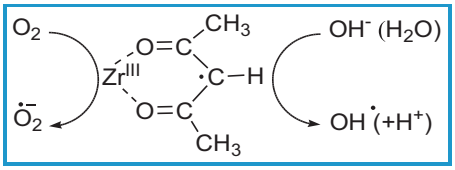

Scheme 3.

stabilized the sol and allowed the formation of a chemically homogeneous gel. The most recent interpretation of this sol stabilization was suggested by Kessler et al. [25] and supported by some recently published papers [26,27]. According to this interpretation, chelating ligands increase the rate of hydrolysis and polycondensation, leading to the formation of nanoparticles formed by oxo-clusters (core) containing *acac* ligands on the surface (shell), that exhibit a structure typical of micelles. The stabilization of sol is obtained as a consequence of the interfacial activity of these micelles [25]. Due to the stability of these complexes, it is expected the *acac* ligands to be still anchored to the zirconium oxo-oligomeric clusters forming the wet gel [28,29], even after the hydrolysis step.

The synthesized ZrO_2-acetylacetonate hybrid material can be described as a polymeric network of zirconium oxo-clusters, on the surface of which part of Zr^{4+} ions are involved in strong complexation with acetylacetonate (*acac*) ligands. In other words, even after drying the HSGZ xerogel holds the acetylacetone used in the sol–gel synthesis and can be considered an *acac* surface-modified porous zirconia [19]. The materials with acetylacetonate zirconium complexes bonded to silica either by one or three Si—O—Zr bonds prepared by Salinier et al. [30] are in some way similar to the HSGZ.

The results of PHE removal tests, above reported, indicate that only the HSGZ material is an active catalyst in the PHE oxidative degradation, while SGZ that does not contain *acac* ligands, is not active as catalyst, even if it can significantly adsorb PHE owing to its high surface area. Therefore, to understand the catalytic activity of HSGZ, the interaction of zirconium with *acac* ligands must be studied.

Ligand-to-metal electron transfer, leading to the formation of free radicals and M^{n-1} derivatives, was first proposed by Arnett and Mendelshon in 1962 [31] as a key step in the autoxidation of iron(III) tris-acetylacetonate ($Fe(acac)_3$). Thereafter many papers reported that several chelates, such as Mn (III), Co (III) acetylacetonate [32,33] or $MoO_2(acac)_2$ [34], yield free radicals and are therefore able to initiate polymerization even at 25 °C [35]. More recently, the formation of free radicals from different transition-metal β-ketoenolates involved in redox reactions was reported, and a number of derived β-ketoenolyl radicals were detected by EPR [36,37]. So, transition-metal acetylacetonate complexes give the formation of free radicals as a consequence of an intramolecular *acac*-to-metal electron transfer process giving M^{n-1}-coordinated *acac*• radicals (Scheme 1).

Analogously, it can be supposed that on the surface of HSGZ material free radicals can be produced by *acac*-to-zirconium electron transfer, giving surface zirconium (III) containing *acac*• radicals in its coordination sphere, according to Scheme 2.

EPR is the reference technique for detection of radicals and more in general of paramagnetic species. Owing to its high sensitivity, EPR is particularly useful in case of surface radical species also when present in very low concentration [38,39]. The EPR spectrum of HSGZ material, recorded at room temperature and shown in Fig. 1, clearly indicates the presence of radical species on the solid surface. In particular, considering the lineshape and g values, the spectrum can be attributed to adsorbed $^{\bullet}O_2^-$ radicals [39,40] that are produced by the contact of HSGZ material with molecular O_2 at room temperature. In the above references superoxide ion radicals are formed only on the surface of ZrO_2 activated by annealing in air or in vacuum at 500–600 °C and then contacted with molecular oxygen at 130 °C [41], while as prepared ZrO_2-acetylacetonate hybrid material (HSGZ) produces $^{\bullet}O_2^-$ at room temperature. Therefore, in the HSGZ material at room temperature *acac*-to-zirconium electron transfer process leads to the coexistence of Zr(IV)-*acac* and Zr(III)-*acac*• complexes in equilibrium at this temperature. Such process can be considered also as a generation of electron/hole pairs (e^-/h^+) in the HSGZ solid material, where the electrons in the conduction band do not belong to specific atoms of the zirconium network but to the solid as a whole.

When HSGZ is used as catalyst in aqueous solution, in the presence of molecular oxygen, reactive oxygen species (ROSs) are produced on its surface, according to Scheme 3.

Alternatively, this can be described as follows:

$$OH^- + acac^{\bullet} \rightarrow acac^- + {}^{\bullet}OH \quad \text{or} \quad OH^- + h^+ \rightarrow {}^{\bullet}OH$$

$$O_2 + Zr(III) \rightarrow Zr(IV) + {}^{\bullet}O_2^- \quad \text{or} \quad O_2 + e^- \rightarrow {}^{\bullet}O_2^-$$

$$^{\bullet}O_2^- + H^+ \rightarrow {}^{\bullet}OOH$$

The molecular oxygen O_2 acting as a conduction band electron scavenger inhibits the fast charge recombination shifting toward right the equilibrium in Scheme 2. The superoxide $^{\bullet}O_2^-$, the hydrogen peroxide •OOH, and the hydroxyl •OH radicals have strong

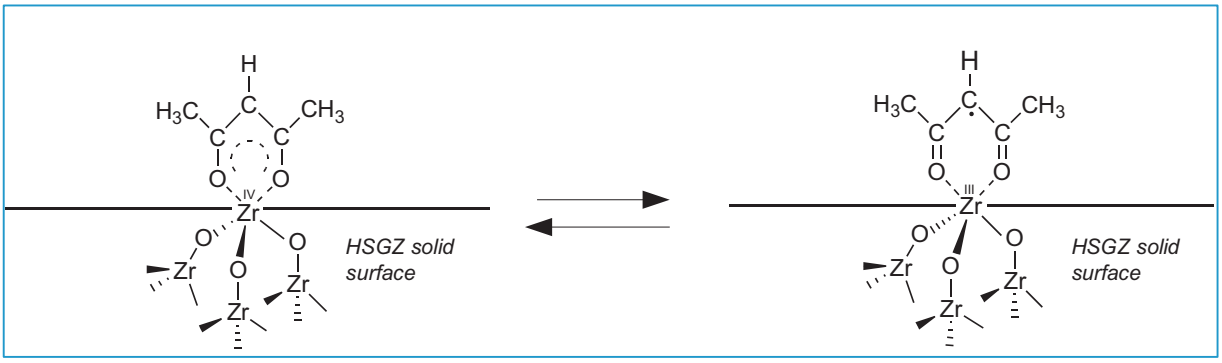

Scheme 2.

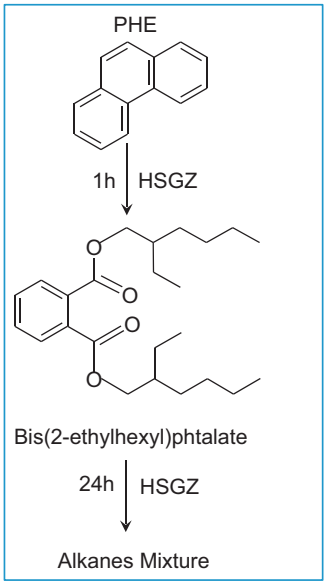

Scheme 4.

oxidation activities and can oxidize or even completely mineralize most organic compounds.

The results of the analysis of the degradation products reported in Figs. 3 and 4 are in agreement with the ones previously reported in the literature, in which phthalates were detected as the main intermediates of phenanthrene photodegradation by TiO_2 under UV irradiation [42,43]. Moreover, the intermediate compounds detected in this study after 1 h incubation time and identified as alkanoic acids, alkanols and alkanes were also observed in previous papers [42,43]. Consequently, it can be inferred that the mechanism summarized in Scheme 4 is acting in both the HSGZ-catalyzed PHE degradation as well as the TiO_2/UV photodegradation.

As reported in the Results section, the SGZ porous material (i.e., gel-derived ZrO_2 without *acac*) is an efficient adsorbent of phenanthrene though it does not catalyse PHE degradation, as testified by the absence of any degradation product. On the contrary, HSGZ porous material acts as heterogeneous catalyst and the percentage removal after 1 h incubation time is higher as the solid/liquid ratio R increases (Fig. 2).

Being the HSGZ a porous material, it can certainly adsorb PHE also before its degradation. Therefore, to study the degradation kinetics, the PHE-removal test described in Fig. 5 was carried out in the presence of HSGZ at $T = 30\,^{\circ}C$, choosing a solid/liquid ratio not too high ($R = 0.4$), so that the effect of the degradation could be appreciably observed before the PHE adsorption was completed.

The PHE-removal kinetic was studied adopting a mechanistic model based on the hypothesis that PHE undergoes reversible first-order adsorption, to be subsequently subjected to chemical degradation, as in the following scheme:

$$C_{sol} \underset{k_{-1}}{\overset{k_1}{\rightleftarrows}} C_{ads} \xrightarrow{k_2} P \tag{3}$$

where C_{ads} indicates the PHE adsorbed, P the degradation products, k_1 and k_{-1} the direct and inverse first-order kinetic constants of the PHE sorption, and k_2 is the first-order kinetic constant of the PHE degradation.

Based on model (3), the following balances on the PHE in solution (C_{sol}) and adsorbed (C_{ads}) could be written:

$$\frac{dC_{sol}}{dt} = -k_1 \times C_{sol} + k_{-1} \times C_{ads} \tag{4}$$

$$\frac{dC_{ads}}{dt} = k_1 \times C_{sol} - (k_{-1} + k_2) \times C_{ads} \tag{5}$$

Solving the system made of the differential Eqs. (4) and (5), a double-exponential mathematical expression was found for the profile $C_{sol}(t)$ similar to that in Eq. (2), as shown in our previous paper [20]. As Eq. (2) had been successfully used to interpolate the kinetic curve in Fig. 5, we adopted the model (3) to explain the PHE-removal mechanism.

The model (3) hypothesizes that PHE can undergo degradation only upon preliminary adsorption. As a matter of facts, no degradation products were observed incubating PHE in the absence of HSGZ catalyst as well as no degradation products were detected when carrying out PHE-removal tests in the presence of a SGZ matrix. In the latter case, the model (3) still provides a reasonable description of the experimental results, yielding a value of the kinetic constant k_2 close to zero. The estimates of the parameters $\lambda_1 = 0.74$ and $\lambda_2 = 9.48 \times 10^{-3}$ values clearly confirm that adsorption process is much faster than degradation.

The industrial application of HSGZ obviously requires an excellent long-term stability of the matrix under applicative conditions. In this view, the achievement of an asymptotic level of PHE removal efficiency after 6 repeated batches (Fig. 6) was a promising result, indicating a stable configuration of the catalyst to be progressively reached, ensuring an excellent resistance to inactivation under continuous operation. It is worth to consider the results reported in Fig. 6 also taking in account that PHE-removal mechanism is based on a preliminary fast adsorption followed by a slower degradation reaction. This means that in the first batch the HSGZ solid is rapidly saturated by PHE therefore in the following batches the removal is due mainly to the degradation reaction.

The stability of the catalyst in the reaction conditions was also testified by the EPR spectra of HSGZ samples after their use in the reaction for 1 h and for a longer one as 24 h. The long contact time gives high progress of the degradation reaction and therefore it assures the affective working of HSGZ as catalyst rather than absorber.

5. Conclusions

For the first time it was shown that a hybrid ZrO_2-acetylacetonate gel-derived material exhibits an intrinsic catalytic activity for the oxidative degradation of PHE in aqueous solution. The prepared HSGZ material behaved like a heterogeneous catalyst, acting as radicals initiator in absence of any light irradiation at 30 °C. Free radicals were formed by an intramolecular *acac*-to-metal electron transfer mechanism giving on the solid surface the equilibrium between Zr(IV)-*acac* and Zr(III)-*acac*$^{\bullet}$ complexes, from which in presence of molecular O_2 reactive oxygen species are produced. The ability of HSGZ material to produce radicalic species was ascertained by EPR spectroscopy. The EPR spectrum was almost unchanged after 1 and 24 h of contact with PHE solution proving the HSGZ stability reaction environment.

The analysis of the degradation products confirmed that the reaction goes on through intermediate free radicals, leading first to the ring opening and the formation of phthalates as main intermediate products. Subsequently low molecular weight alkanes and final mineralization products were formed.

A two-steps model was proposed to describe the kinetics of PHE removal, based on a fast, initial adsorption of PHE on the HSGZ catalyst, followed by its chemical degradation.

Finally, the catalyst retained most of its catalytic activity in repeated tests under reaction conditions, reaching a stable level of PHE removal efficiency.

References

[1] Y.Z. Gao, L.Z. Zhu, Chemosphere 55 (2004) 1169–1178.
[2] Y. Yang, F. Hildebrand, Anal. Chim. Acta 55 (2006) 364–369.
[3] K.L. Shuttleworth, C.E. Cerniglia, Microb. Ecol. 31 (1996) 305–317.
[4] M.A. Nkansah, A.A. Christy, T. Barth, G.W. Francis, J. Hazard. Mater. 360 (2012) 217–218.
[5] B. Mahanty, K. Pakshirajan, V.V. Dasu, Crit. Rev. Environ. Sci. Technol. 41 (2011) 1697–1746.
[6] S.M. Bamforth, I. Singleton, J. Chem. Technol. Biotechnol. 80 (2005) 723–736.
[7] A.K. Haritash, C.P. Kaushik, J. Hazard. Mater. 169 (2009) 1–15.
[8] L. Levin, A. Viale, A. Forchiassin, Int. Biodeterior. Biodegrad. 52 (2003) 1–5.
[9] T.G. Reichenauer, J.J. Germida, Chem. Sus. Chem. 1 (2008) 708–717.
[10] H.H. Huang, D.H.L. Tseng, C. Juang, J. Hazard. Mater. 156 (2008) 186–193.
[11] R. Molinari, F. Pirillo, V. Loddo, L. Palmisano, Catal. Today 118 (2006) 205–213.
[12] A. Fujishima, T.N. Tao, D.A. Tryk, J. Photochem. Photobiol. C 1 (2000) 1–21.
[13] J. Kou, Z. Li, Y. Yuan, H. Zhang, Y. Wang, Z. Zou, Environ. Sci. Technol. 43 (2009) 2919–2924.
[14] S.W. Chang Chien, C.H. Chang, S.H. Chen, M.C. Wang, M. Madhava Rao, S. Satya Veni, Sci. Total Environ. 409 (2011) 4101–4108.
[15] M.J. Garcia-Martinez, L. Canora, G. Blazquez, I. Da Riva, R. Alcantara, J.F. Llamas, Chem. Eng. J. 110 (2005) 123–128.
[16] A.L. Linsebigler, G. Lu, J.T. Jr. Yates, Chem. Rev. 95 (1995) 735-758.
[17] M.A. Heitkamp, C.E. Cerniglia, Appl. Environ. Microbiol. 54 (1988) 1612–1614.
[18] A.R. Mesdhaghinia, S. Nasseri, M. Arbabi, S. Rezaie, Proc. of the 9th Int. Conf. on Environment Science and Technology, 1–3 Sept., Rhodes, Greece, 2005, pp. A-984–A-991.
[19] A. Aronne, F. Sannino, S.R. Bonavolontà, E. Fanelli, A. Mingione, P. Pernice, R. Spaccini, D. Pirozzi, Environ. Sci. Technol. 46 (2012) 1755–1763.
[20] F. Sannino, D. Pirozzi, A. Aronne, E. Fanelli, R. Spaccini, A. Yousuf, P. Pernice, Environ. Sci. Technol. 44 (2010) 9476–9481.
[21] D. Pirozzi, E. Fanelli, A. Aronne, P. Pernice, A. Mingione, J. Mol. Catal. B-Enzym. 59 (2009) 116–120.
[22] L. Panzella, G. Gentile, G. D'Errico, N.F. Della Vecchia, M.E. Errico, A. Napolitano, C. Carfagna, M. d'Ischia, Angew. Chem. Int. Ed. 52 (2013) 12684–12687.
[23] G.I. Spijksma, H.J.M. Bouwmeester, D.H.A. Blank, V.G. Kessler, Chem. Commun. 16 (2004) 1874–1875.
[24] G.A. Seisenbaeva, S. Gohil, V.G. Kessler, J. Mater. Chem. 14 (2006) 3177–3190.
[25] V.G. Kessler, G.I. Spijksma, G.A. Seisenbaeva, S. Håkansson, D.H. Blank, H.J.M. Bouwmeester, J. Sol–Gel Sci. Technol. 40 (2006) 163–179.
[26] S. Lemonnier, S. Grandjean, A.C. Robisson, J.P. Jolivet, Dalton Trans. 39 (2010) 2254–2262.
[27] C.R. Van de Brom, N. Vogel, C.P. Hayser, S. Goerres, M. Wagner, K. Landfester, C.K. Weiss, Langmuir 27 (2011) 8044–8053.
[28] C. Sanchez, M. In, J. Non-Cryst. Solids 147–148 (1992) 1–12.
[29] M.J. Percy, J.R. Barlett, J.L. Woolfrey, L. Spiccia, B.O. West, J. Mater. Chem. 9 (1999) 499–505.
[30] V. Salinier, J.M. Corker, F. Lefebvre, F. Bayard, V. Dufaud, J.M. Basseta, Adv. Synth. Catal. 351 (2009) 2155–2167.
[31] E.M. Arnett, M.A. Mendelsohn, J. Am. Chem. Soc. 84 (1962) 3824–3829.
[32] C.H. Bamford, A.N. Ferrar, Proc. R. Soc. 321 (1971) 425–443.
[33] C.H. Bamford, D.J. Lind, Proc. R. Soc 302 (1968) 145–165.
[34] Y. Nishikawa, T. Otsu, Makromol. Chem. 129 (1969) 276–278.
[35] C.H. Bamford, A.N. Ferrar, Chem. Commun. (1970) 315–316.
[36] C.L. Kwan, J.K. Kochi, J. Am. Chem. Soc. 98 (1976) 4903–4912.
[37] M. Bruni, P. Diversi, G. Ingrosso, A. Lucherini, C. Pinzino, A. Raffaelli, J. Chem. Soc. Dalton Trans. (1995) 1035–1041.
[38] J.A. Weil, J.R. Bolton, J.E. Wertz, Electron Spin Resonance, Second ed., Ellis Horwood, New York, 1993.
[39] E. Cesareo, L. Korkina, G. D'Errico, G. Vitiello, M.S. Aguzzi, F. Passarelli, J.Z. Pedersen, A. Facchiano, Plos One 7 (2012) e48849.
[40] A.F. Bedilo, M.A. Plotnikov, N.V. Mezentseva, A.M. Volodin, G.M. Zhidomirov, I.M. Rybkin, K.J. Klabunde, Phys. Chem. Chem. Phys. 7 (2005) 3059–3069.
[41] C. Gionco, M.C. Paganini, E. Giamello, R. Burgess, C. Di Valentin, G. Pacchioni, Chem. Mater. 25 (2013) 2243–2253.
[42] Y. Zhang, J.W.C. Wong, L. Peihong, Y.J. Min, Hazard. Mater. 191 (2011) 136–143.
[43] H. Jia, J. Zhao, X. Fan, K. Dilimulati, C. Wang, Appl. Catal. B-Environ. 123 (2012) 43–51.